Journal of Environmental Management 415 (2026) 130715

Contents lists available at ScienceDirect

Journal of Environmental Management

journal homepage: www.elsevier.com/locate/jenvman

Research article

# Seasonal variations and anthropogenic dredging drive dominant mechanism shifts in phosphorus retention in agricultural drainage ditches

Jiahui Wang [a,b], Minghong Chen [a,b,*], Minghui Qiu [a,b], Fengchu Wang [a,b], Xuanye Liu [a,b], Chaozi Wang [a,b], Zailin Huo [a,b]

[a] State Key Laboratory of Efficient Utilization of Agricultural Water Resources, China Agricultural University, Beijing, 100083, China
[b] Center for Agricultural Water Research in China, China Agricultural University, Beijing, 100083, China

ARTICLE INFO

*Keywords:*
Agricultural drainage ditches
Channel conditions
Vegetation
Dredging
Phosphorus retention
OTIS

ABSTRACT

Although channel conditions in agricultural drainage ditches vary substantially with seasonal changes and dredging activities, their effects on phosphorus retention mechanisms remain poorly understood. This study combined tracer experiments with the One-dimensional Transport with Inflow and Storage (OTIS) model to investigate phosphorus retention under different channel conditions in the Fourth Main Drainage Ditch of the Hetao Irrigation District, China. Results showed that from summer to autumn and into the spring following dredging, the overall retention rate of soluble reactive phosphorus (SRP) decreased, while the contribution of the main channel increased progressively and became dominant. During periods with dense vegetation and a well-developed storage zone, biological uptake and assimilation likely played a major role in phosphorus retention. In contrast, reduced vegetation cover, increased flow velocity, and alterations in channel ecological structure following dredging may have contributed to the decline in phosphorus retention capacity and the increased contribution of the main channel, while enhancing the relative importance of adsorption processes. These findings suggest that seasonal variations and anthropogenic dredging can influence phosphorus retention patterns and modify the relative importance of different retention mechanisms in agricultural drainage ditches. The results highlight the importance of maintaining ecological storage functions and provide a scientific basis for optimizing ditch management, improving water quality, and mitigating agricultural nonpoint-source pollution.

## 1. Introduction

Globally, freshwater ecosystems face persistent challenges of water quality degradation and biodiversity loss, with eutrophication recognized as one of the most critical threats (Giri, 2021; Ho et al., 2019; Reid et al., 2019). Decades of intensive phosphate fertilizer use have led to phosphorus accumulation in agricultural soils, increasing the risk of phosphorus transfer to aquatic systems. Consequently, agricultural non-point source pollution has become a major contributor to phosphorus loading in freshwater bodies and a key driver of eutrophication (Conley et al., 2009; Ji et al., 2024; K. Zhang et al., 2025). From a biogeochemical perspective, this process is also constrained by stoichiometric coupling of carbon, nitrogen, and phosphorus across terrestrial–aquatic interfaces (Liu et al., 2023). Agricultural drainage ditches serve act as primary conduits linking farmland with downstream water bodies such as wetlands, rivers, and lakes (Bieroza et al., 2024). These ditches play a crucial role in intercepting and transforming phosphorus during its transport (Li et al., 2021; Zhang et al., 2024). Therefore, elucidating phosphorus retention and transport processes in these ditches is essential for developing strategies to mitigate agricultural non-point source pollution and control downstream eutrophication (Hu et al., 2026).

Agricultural drainage ditches are complex ecosystems composed of water, vegetation, sediments, and microorganisms. They function not only as hydraulic conduits but also as biologically active systems with important ecological regulatory roles. Growing evidence indicates that drainage ditches can intercept and retain phosphorus through multiple mechanisms, including plant uptake, sediment adsorption, and microbial assimilation via biofilms (Karl, 2014; Nsenga Kumwimba et al., 2018; Vymazal and Březinová, 2018). Although these mechanisms have been widely studied, most existing research has focused on individual processes within specific ecological components or under controlled, site-specific conditions, limiting a comprehensive understanding of phosphorus retention at the whole-ditch scale (Chen et al.,

* Corresponding author. State Key Laboratory of Efficient Utilization of Agricultural Water Resources, China Agricultural University, Beijing 100083, China.
*E-mail address:* chenminghong@cau.edu.cn (M. Chen).

https://doi.org/10.1016/j.jenvman.2026.130715
Received 5 February 2026; Received in revised form 19 June 2026; Accepted 11 August 2026
Available online 15 August 2026
0301-4797/© 2026 Elsevier Ltd. All rights are reserved, including those for text and data mining, AI training, and similar technologies.

2022; De Oliveira et al., 2024; Gao et al., 2024; H. Li et al., 2025 ). In fact, phosphorus retention results from the combined effects of vegetation, sediments, microorganisms, and hydrodynamic processes, and is therefore highly sensitive to changes in channel conditions and broader biogeochemical constraints (Cui et al., 2020; C. Li et al., 2025).

Among the factors influencing drainage ditch conditions, seasonal variation and dredging are particularly important (Bukaveckas, 2007; Moore et al., 2017). Seasonal variation affects phosphorus transport and retention by regulating vegetation growth, microbial activity, and hydrological processes. Dredging, a common management practice in agricultural drainage ditches, restores channel conveyance and drainage capacity while also improving water quality (Riza et al., 2023). However, dredging can substantially alter ecological and hydrodynamic conditions through vegetation removal, sediment disturbance, biofilm disruption, and channel reshaping (Xiang et al., 2024). These changes may modify flow dynamics and solute exchange processes (J. Zhang et al., 2025; Zhao et al., 2024), ultimately affecting phosphorus retention pathways (Shigaki et al., 2008).

Phosphorus retention in drainage ditches exhibits pronounced spatial heterogeneity, occurring non-uniformly along the channel and being strongly governed by hydrodynamic patterns. To represent this process, the Transient Storage Model (TSM) was developed (Bencala and Walters, 1983). The One-dimensional Transport with Inflow and Storage (OTIS) model was developed on this basis, and has been widely applied to small-scale river systems, including drainage ditches (Harvey et al., 1996; Runkel, 1998). The OTIS model conceptualizes the channel as two zones: the main channel, characterized by relatively rapid flow, and the storage zone, with near-zero velocity and extended residence time. Solute exchange between these zones occurs through transient storage processes. It has been widely used to characterize spatial heterogeneity in nutrient transport and retention in drainage ditches (Field et al., 2023; Gooseff et al., 2007; Liu et al., 2022). Studies have shown that channel morphology, flow conditions, and vegetation density directly influence the area ratio and the exchange rates between the main channel and storage zone, thereby affecting nutrient retention efficiency (Harvey and Gooseff, 2015; Zarnetske et al., 2007).

Within the OTIS framework, phosphorus retention can be simplified into three primary processes: biological uptake and assimilation, adsorption, and hydrological processes (Liu et al., 2022; Runkel et al., 1996). Previous studies have highlighted the important role of biological uptake and assimilation in phosphorus retention in both the main channel and storage zone (Runkel et al., 1996). However, quantitative comparisons of the relative contributions of these two zones under channel conditions altered by seasonal variation and anthropogenic dredging remain limited (Field et al., 2023).

To address these issues, this study aims to: (1) quantify the effects of seasonal variations and dredging-induced channel modifications on phosphorus retention rates and the relative contributions of the main channel and the storage zone; (2) elucidate shifts in dominant phosphorus retention mechanisms under different channel conditions; and (3) provide a scientific basis for the optimized management and ecological restoration of agricultural drainage ditches.

## 2. Materials and methods

### 2.1. Site description

The study area is located in the Hetao Irrigation District (HID), Inner Mongolia Autonomous Region, China. This region is a typical arid to semi-arid agricultural area with low precipitation, where crop production depends primarily on water diverted from the Yellow River. The district comprises approximately 103,600 irrigation and drainage canals organized into seven hierarchical levels. Between 2022 and 2024, the average annual fertilizer application reached $4.04 \times 10^8$ kg (as pure nutrient). Prolonged high fertilizer inputs, coupled with inefficient irrigation practices, have exacerbated non-point source pollution in the region.

In this study, a 107 m reach of the Fourth Main Drainage Ditch in the middle-to-lower reaches of the HID was selected as the experimental site (Fig. 1). The selected reach is straight with no meanders. Surface sediments (0-10 cm) are dominated by silt (67.8%) and sand (26.8%) and are classified as silty loam according to the American System of Soil Texture Classification (ASSC). Three experiments were conducted on 15 August 2024 (SFI: the fifth irrigation event, occurring in summer), 16 November 2024 (ASI: the sixth irrigation event, occurring in autumn), and 30 May 2025 (SSI: the second irrigation event, occurring in spring). Hydrological and ecological conditions varied among the three periods. (1) SFI: Water temperature was 26.8 °C. Reeds were dense and evenly distributed along both ditch banks, and flow velocity was relatively low (Fig. 2a). (2) ASI: Water temperature dropped to 4.2 °C. Reeds had senesced, and flow velocity remained low (Fig. 2b). (3) SSI: Water temperature was 19.1 °C; the ditch had been dredged prior to the experiment, leaving only sparse reed seedlings and a few submerged plants. Channel width and depth were reduced, resulting in enhanced conveyance capacity and significantly higher flow velocity (Fig. 2c).

### 2.2. Experiments

In all three experiments, NaBr was used as a conservative tracer, and $KH_2PO_4$ as the nutrient tracer. Before each experiment, basic hydrological parameters, including flow velocity, water surface width, depth, and temperature, were measured along the ditch reach. In addition, overlying water samples were collected from both the main channel and vegetated zones at each sampling site to determine the background concentrations of bromide ($Br^-$) and soluble reactive phosphorus (SRP).

Based on the flow velocity and background concentrations measured prior to each experiment, 1000 g, 5000 g, and 2500 g of NaBr and $KH_2PO_4$ were applied during SFI, ASI, and SSI, respectively. Both tracers were dissolved in ditch water and instantaneously injected at injection site A. Four downstream sampling sites (B–E) were located 5 m, 27 m, 71 m, and 107 m downstream of the injection site, respectively (Fig. 1). After tracer injection, electrical conductivity was continuously monitored at each sampling point using a portable conductivity meter (CT-20, LICHEN Scientific Instruments, Shanghai, China) to determine sampling frequency and define the end of each experiment. Sampling was terminated when conductivity returned to background levels.

Water samples were collected in 80 mL PET bottles, labeled, and immediately transported to the laboratory. Samples were stored at −4 °C until analysis. Prior to analysis, all samples were filtered through 0.45 μm nylon syringe filters. $Br^-$ concentrations were measured using a bromide ion-selective electrode equipped with a Thermo Scientific Orion Star A214 pH/ISE meter (Thermo Fisher Scientific Inc., Waltham, MA, USA), and SRP concentrations were determined with an AA3 Continuous Flow Analyzer (SEAL Analytical GmbH, Norderstedt, Germany) following the acid molybdenum blue colorimetric method.

### 2.3. OTIS model and parameters

#### 2.3.1. OTIS model

Experiment data were simulated using the OTIS model developed by the U.S. Geological Survey (USGS) (Runkel, 1998). The OTIS model is designed for simulating solute transport and transformation in small streams (e.g., headwater streams, drainage ditches). It accounts for processes including advection–dispersion, transient storage, biological uptake and assimilation (represented by first-order decay), adsorption, and lateral inflow (Eqs. (1)–(3)). In this study, lateral inflow was assumed to be negligible. The model conceptualizes the channel as two compartments: a main channel and a storage zone. Solute exchange occurs between these compartments through transient storage processes. The details of the model are described in Supplementary Material "Text S1. OTIS model details".

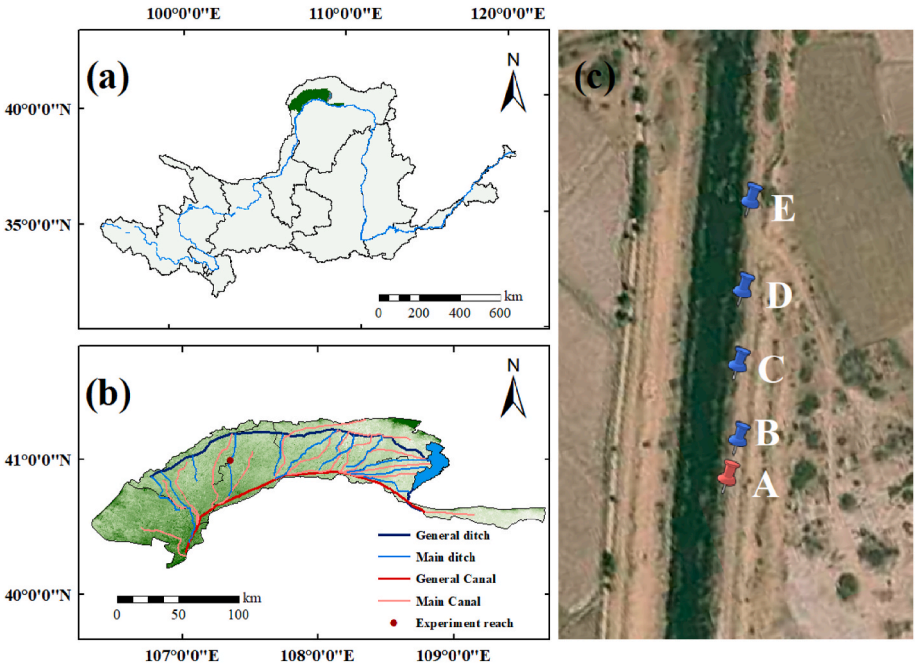


**Fig. 1.** Overview of the study area. (a) Location of the Hetao Irrigation District (dark green area) within the Yellow River Basin; (b) location of the experimental ditch section (red point) within the Hetao Irrigation District; (c) injection site (A) and sampling sites (B–E) within the experimental ditch section.

**Fig. 2.** Channel conditions at different periods. Panels: (a) SFI (the fifth irrigation event, occurring in summer), (b) ASI (the sixth irrigation event, occurring in autumn), (c) SSI (the second irrigation event, occurring in spring).

$$\frac{\partial C}{\partial t} = -\frac{Q}{A}\frac{\partial C}{\partial x} + \frac{1}{A}\frac{\partial}{\partial x}\left(AD\frac{\partial C}{\partial x}\right) + \frac{q_{Lin}}{A}(C_L\text{-}C) + \alpha(C_s\text{-}C) + \rho\widehat{\lambda}(C_{sed}\text{-}K_dC)\text{-}\lambda C \quad (1)$$

$$\frac{dC_s}{dt} = \alpha\frac{A}{A_s}(C\text{-}C_s) + \widehat{\lambda}_s(\widehat{C}_s\text{-}C_s)\text{-}\lambda_s C_s \quad (2)$$

$$\frac{dC_{sed}}{dt} = \widehat{\lambda}(K_dC\text{-}C_{sed}) \quad (3)$$

Where $C$ is the solute concentration in the main channel (mg $L^{-1}$), $C_L$ is the solute concentration of the lateral inflow (mg $L^{-1}$), $C_s$ is the solute concentration in the storage zone (mg $L^{-1}$), $\widehat{C}_s$ is the background solute concentration in storage zone (mg $L^{-1}$), $C_{sed}$ is the sorbate concentration on the streambed sediment (mg $mg^{-1}$), $Q$ is the volumetric flow rate ($m^3$ $s^{-1}$), $A$ is the cross-sectional area of the main channel ($m^2$), $As$ is the cross-sectional area of the storage zone ($m^2$), $D$ is the dispersion coefficient ($m^2$ $s^{-1}$), $\alpha$ is the storage zone exchange coefficient ($s^{-1}$), $q_{Lin}$ is the lateral inflow rate ($m^2$ $s^{-1}$), $\lambda$ is the main channel first-order decay coefficient ($s^{-1}$), $\lambda_s$ is the storage zone first-order decay coefficient ($s^{-1}$), $\widehat{\lambda}$ is the main channel sorption rate coefficient ($s^{-1}$), $\widehat{\lambda}_s$ is the storage zone sorption rate coefficient ($s^{-1}$), $\rho$ is the mass of accessible sediment/volume water (mg $L^{-1}$), $K_d$ is the distribution coefficient (L $mg^{-1}$), $t$ is the time (s), $x$ is the distance (m).

### 2.3.2. Inverse modeling

During model calibration, the concentration-time curves of $Br^-$ and SRP at sampling site B were used as upstream boundary conditions to ensure accurate model input. Hydrological parameters ($Q$, $A$, $As$, $D$ and $\alpha$) were determined first, with $Q$ obtained directly from field measurements. The remaining hydrological parameters ($A$, $As$, $D$ and $\alpha$) were sequentially calibrated at sampling sites C, D, and E using $Br^-$ breakthrough curves. During this calibration, the reaction terms in Eqs. (1) and (2) were omitted, thereby excluding adsorption and biological uptake and assimilation as biogeochemical processes.

After the hydrological parameters had been determined, the SRP breakthrough curves at sampling sites C, D, and E were used to calibrate the non-hydrological parameters ($\lambda$, $\widehat{\lambda}$, $\lambda_s$, $\widehat{\lambda}_s$). Parameter values were refined iteratively to obtain the best agreement between simulated and observed breakthrough curves. Further details regarding parameter estimation are provided in the Supplementary Material (Text S2. Inverse modeling details).

### 2.3.3. SRP retention potential indicators

Following calibration of the hydrological parameters, several metrics describing the SRP retention potential of the drainage ditch were derived (Harvey et al., 1996; Harvey and Wagner, 2000; Runkel, 2002). These include: (1) main channel residence time ($T_c$, s), defined as the average time SRP remains in the main channel before entering the storage zone; (2) storage zone residence time ($T_s$, s), representing the average time SRP remains in the storage zone; (3) main channel

conservative spiraling length ($L_s$, m), representing the average distance that SRP travels downstream within the main channel prior to entering the storage zone; (4) hydrological retention factor ($R_h$, s·m$^{-1}$), representing the average residence time of solutes in the storage zone per unit length of the drainage ditch; (5) storage exchange flux ($q_s$, m$^3$·s$^{-1}$·m$^{-1}$), representing the average water flux through the storage zone per unit length. The corresponding equations are provided in Table 2.

### 2.4. Calculation of SRP retention rate and contribution share by zone

Based on the simulation results of the OTIS model, SRP retention in the main channel and the storage zone was quantified separately. The model output the SRP concentrations in both zones. Here, $i$ denotes the discrete spatial unit (1 m per unit), and $j$ denotes the time step. Using these variables, the SRP exchange flux ($q_i(t)$), the amount of SRP entering the storage zone ($M_{s'in}$), the release ($M_{s'out}$), and the net retention ($M_s$) can be expressed by Eqs. (4)–(7), respectively.

$$q_i(t) = \alpha \cdot A\left(C_i(t) - C_{s,i}(t)\right) \tag{4}$$

$$M_{s'in} = \sum_{i=1}^{L}\sum_{j=1}^{N} \max(q(x,t),0)\Delta x \Delta t \tag{5}$$

$$M_{s'out} = \sum_{i=1}^{L}\sum_{j=1}^{N} \max(-q(x,t),0)\Delta x \Delta t \tag{6}$$

$$M_s = M_{s'in} - M_{s'out} \tag{7}$$

The total mass of SRP passing through the upstream and downstream boundaries of the ditch reach was calculated using Eqs. (8) and (9), respectively. The total SRP retention in the ditch reach ($M_r$) was then calculated as the difference between these two values (Eq. (10)). SRP retention in the main channel ($M_m$) was subsequently calculated using Eq. (11).

$$M_{in} = Q\int_0^t C_1(t)dt \tag{8}$$

**Table 1**
Measured and OTIS-calibrated hydrological parameters.

| Hydrological parameters of ditches | SFI | ASI | SSI |
|---|---|---|---|
| Water surface width $W$[a](m) | 12.53 ± 1.05 | 13.80 ± 0.20 | 11.73 ± 0.19 |
| Water depth at the channel center $h$[a](m) | 1.47 ± 0.05 | 1.67 ± 0.02 | 1.00 ± 0.05 |
| Cross-sectional area of the main channel $A$[b] (m$^2$) | 7.77 ± 1.78 | 10.60 ± 2.69 | 7.17 ± 1.37 |
| Cross-sectional area of the storage zone $As$[b] (m$^2$) | 6.27 ± 0.77 | 4.00 ± 0.08 | 2.03 ± 0.56 |
| areal proportion of storage zone [$As/(A + As)$][c] | 0.45 ± 0.09 | 0.28 ± 0.05 | 0.22 ± 0.02 |
| Dispersion coefficient $D$[b] (m$^2$/s) | 0.013 | 0.010 | 0.160 |
| Exchange coefficient $\alpha$[b] (×10$^{-4}$s$^{-1}$) | 2.27 ± 1.51 | 0.97 ± 0.21 | 7.07 ± 2.45 |
| Volumetric flow rate $Q$[a] (m$^3$ s$^{-1}$) | 0.14 | 0.19 | 0.60 |
| Flow velocity [$v = Q/A$ ] (m s$^{-1}$) | (0.019 ± 0.005)[c] | (0.019 ± 0.004)[c] | (0.087 ± 0.015)[d] |

[a] Measured values.
[b] Parameters calibrated using the trial-and-error method.
[c] Calculated from calibrated parameters.
[d] Calculated from both calibrated and measured parameters.

**Table 2**
SRP retention potential indicators of drainage ditches.

| SRP retention potential indicators | SFI | ASI | SSI |
|---|---|---|---|
| Main channel residence time [$T_c = 1/\alpha$] (min) | 123 ± 84 | 181 ± 42 | 27 ± 11 |
| Storage zone residence time [$T_s = A_s/(\alpha A)$] (min) | 93 ± 44 | 70 ± 11 | 7 ± 2 |
| Main channel conservative spiraling length [$L_s = Q/(\alpha A)$] (m) | 130 ± 69 | 198 ± 30 | 148 ± 74 |
| hydrological retention factor [$R_h = T_s/L_s = A_s/Q$] (s m$^{-1}$) | 44.8 ± 5.5 | 21.1 ± 0.4 | 3.4 ± 0.9 |
| storage exchange flux [ $q_s = \alpha A$] (×10$^{-4}$ m$^2$ s$^{-1}$) | 17.3 ± 12.8 | 9.8 ± 1.4 | 53.6 ± 27.8 |

$$M_{out} = Q\int_0^t C_2(t)dt \tag{9}$$

$$M_r = M_{in} - M_{out} \tag{10}$$

$$M_m = M_R - M_s \tag{11}$$

Where $C_1(t)$ and $C_2(t)$ denote the SRP concentrations at the upstream and downstream boundaries of the ditch reach, respectively.

The overall SRP retention rate in each ditch reach ($P_r$), the retention rates in the main channel and the storage zone ($P_{m1}$ and $P_{s1}$), and the relative contributions of the main channel and the storage zone to total SRP retention ($P_m$ and $P_s$) were calculated using Eqs. (12)–(16).

$$P_r = \frac{M_r}{M_{in}} \times 100\% \tag{12}$$

$$P_{m1} = \frac{M_m}{M_{in}} \times 100\% \tag{13}$$

$$P_{s1} = \frac{M_m}{M_{in}} \times 100\% \tag{14}$$

$$P_m = \frac{M_m}{M_r} \times 100\% \tag{15}$$

$$P_s = \frac{M_s}{M_r} \times 100\% \tag{16}$$

### 2.5. Quantifying the contributions of different mechanisms to SRP retention

To quantify the contributions of adsorption, biological uptake and assimilation, and hydrological processes to SRP retention in the main channel and the storage zone, three simulation scenarios were developed (McKnight et al., 2004; Runkel, 2007).

Scenario 1: Included advection–dispersion, transient storage, biological uptake and assimilation, and adsorption.

Scenario 2: Same as Scenario 1, but with adsorption disabled ($\widehat{\lambda} = \widehat{\lambda}_s = 0$).

Scenario 3: Same as Scenario 1, but with biological uptake and assimilation disabled ($\lambda = \lambda_s = 0$).

All scenarios were modifications of the original OTIS model. Using these simulations, the SRP retention amounts in the main channel, the storage zone, and the total retention for the BE ditch reach were calculated as $M_{tm,total}$, $M_{tm,biotic}$, $M_{tm,sorb}$, $M_{ts,total}$, $M_{ts,biotic}$, $M_{ts,sorb}$, $M_{tr,total}$, $M_{tr,biotic}$, $M_{tr,sorb}$, respectively.

The contributions of adsorption ($P_{m,sorb}$), biological uptake and assimilation ($P_{m,biotic}$), and hydrological processes ($P_{m,hyd}$) to SRP retention in the main channel were calculated using Eqs. (17)–(19), whereas the corresponding contributions in the storage zone ($P_{s,sorb}$, $P_{s,biotic}$ and $P_{s,hyd}$) were calculated using Eqs. (20)–(22).

$$P_{m,sorb} = \frac{M_{tm,total} - M_{tm,biotic}}{M_{tr,total}} \times 100\% \quad (17)$$

$$P_{m,biotic} = \frac{M_{tm,total} - M_{tm,sorb}}{M_{tr,total}} \times 100\% \quad (18)$$

$$P_{m,hyd} = \frac{M_{tm,total} - \left(M_{tm,total} - M_{tm,biotic}\right) - \left(M_{tm,otal} - M_{tm,sorb}\right)}{M_{tr,total}} \times 100\% \quad (19)$$

$$P_{s,sorb} = \frac{M_{ts,total} - M_{ts,biotic}}{M_{tr,total}} \times 100\% \quad (20)$$

$$P_{s,biotic} = \frac{M_{ts,total} - M_{ts,sorb}}{M_{tr,total}} \times 100\% \quad (21)$$

$$P_{s,hyd} = \frac{M_{ts,total} - \left(M_{ts,total} - M_{ts,biotic}\right) - \left(M_{ts,total} - M_{ts,sorb}\right)}{M_{tr,total}} \times 100\% \quad (22)$$

## 3. Results

### 3.1. $Br^-$ and SRP transport in ditches

The three experiments yielded relative concentration breakthrough curves for $Br^-$ and SRP at sampling sites C, D, and E. Relative concentration was defined as the ratio of concentration at each sampling site to the maximum concentration (sampling site B,$C_{B'max}$). Simulated relative concentration breakthrough curves were generated using the OTIS model. Good agreement was observed between simulated and measured results, indicating that the model successfully captured the observed concentration dynamics. The coefficients of determination ($R^2$) ranged from 0.602 to 0.822, and Nash–Sutcliffe efficiency (NSE) values ranged from 0.511 to 0.734 (Fig. 3).

$Br^-$ served as a conservative tracer to characterize water transport within the drainage ditch. During SFI and ASI, $Br^-$ transport was prolonged and characterized by gradual concentration declines and pronounced tailing. Peak arrival times at each sampling site were largely consistent between the two periods (Fig. 3a and c). In contrast, breakthrough curves during SSI were markedly sharper, with rapid post-peak

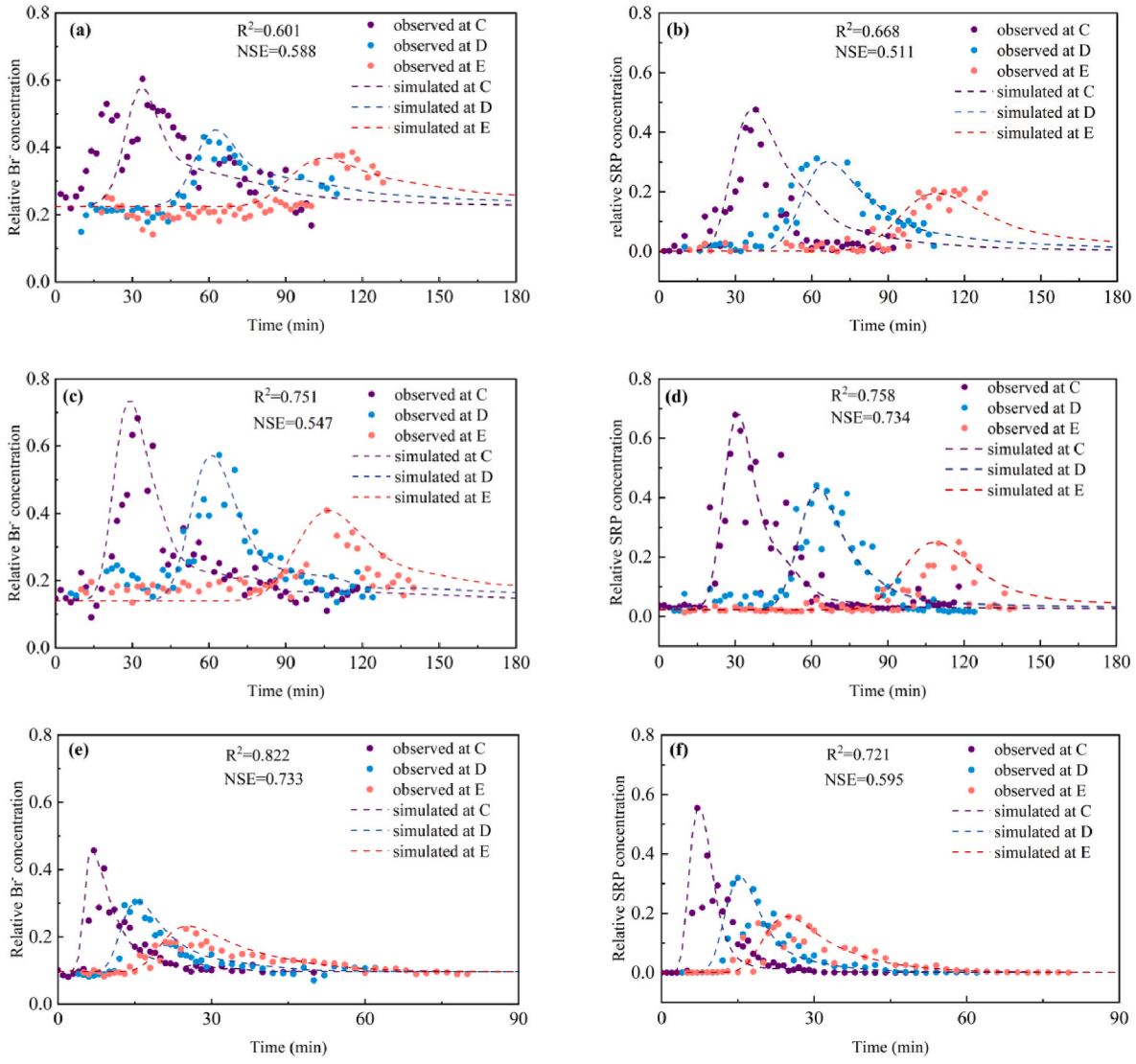


**Fig. 3.** Measured and simulated relative concentration breakthrough curves of $Br^-$ and SRP at sampling sites C, D, and E. The values represent the ratio of the concentration ($C$) at each sample site to the maximum concentration observed at the upstream boundary ($C_{B'max}$). Panels (a), (c), and (e) show $Br^-$ results for SFI (the fifth irrigation event, occurring in summer), ASI (the sixth irrigation event, occurring in autumn), and SSI (the second irrigation event, occurring in spring), respectively, while panels (b), (d), and (f) show the corresponding SRP results.

declines, minimal tailing, and substantially earlier peak arrivals at all sampling sites (Fig. 3e). Declines in relative $Br^-$ peak concentrations between consecutive sampling sites varied among periods and showed no consistent trend (SFI: 28%, 13%; ASI: 16%, 29%; SSI: 33%, 26%). Relative SRP concentration patterns generally mirrored those of $Br^-$ across all periods. However, due to non-conservative retention processes, reductions in SRP peak concentrations at sampling sites D and E were substantially greater than those observed for $Br^-$ (SFI: 34%, 34%; ASI: 35%, 43%; SSI: 49%, 41%).

Simulated relative SRP breakthrough curves in the main channel and the storage zone at sampling sites C, D, and E are shown in Fig. 4. The results indicated that SRP exchange between the two zones was bidirectional and driven by concentration gradients, rather than occurring solely from the main channel to the storage zone. During SFI and ASI, SRP responses in the storage zone lagged behind those in the main channel, and concentrations declined gradually after reaching peak values, suggesting that SRP remained in the storage zone for extended periods before being slowly released back to the main channel. In contrast, during SSI, the storage zone response occurred much earlier, reaching equilibrium with the main channel within 30 min and a new equilibrium state within 90 min. These findings suggest that SRP exchange between the two zones was more rapid and pronounced during SSI.

### 3.2. Differences in hydrological parameters and SRP retention potential indicators

The hydrological parameters of the drainage ditch are summarized in Table 1. Among the three study periods, ASI exhibited the greatest water surface width, depth, and total cross-sectional area ($A + As$), whereas SSI (post-dredging) showed the smallest values. During SFI, dense vegetation growth (e.g., reeds) resulted in a high storage zone proportion (0.45), which decreased during ASI as vegetation senesced and declined further during SSI following dredging. Flow velocities ($v$) during SFI and ASI were nearly identical (0.019 m $s^{-1}$), consistent with the similar peak arrival times observed in the two periods (Section 3.1). Despite having the smallest flow-carrying cross-sectional area, SSI exhibited the highest $Q$ (0.60 $m^3$ $s^{-1}$) and $v$ (0.087 m $s^{-1}$), primarily due to channel reshaping and reduced hydraulic roughness following dredging. Dredging increased water conveyance per unit area, enhanced exchange between the main channel and the storage zone, and accelerated $Br^-$ and SRP transport. Consequently, both the $\alpha$ ($7.07\times10^{-4}$ $s^{-1}$) and $D$ (0.160 $m^2$ $s^{-1}$) reached their maximum values during SSI.

Detailed information on non-hydrological parameters is provided in the Supplementary Material "Text S3. Model parameter details". In addition, a sensitivity analysis was conducted to evaluate the robustness of the model and the influence of key hydrological and non-hydrological parameters on simulation results; the methodology and results are presented in Supplementary Material (Text S4. Sensitivity analysis).

The SRP retention potential indicators for the drainage ditch are summarized in Table 2. $T_c$ reached its highest value during ASI (181 min) but declined sharply to its minimum during SSI (27 min). Similarly, $L_s$ peaked in ASI (198 m), suggesting greater SRP retention potential within the main channel under ASI conditions. In contrast, the storage zone exhibited the highest $T_s$ (93 min) and $R_h$ (44.8 s $m^{-1}$) during SFI, followed by ASI (70 min, 21.1 s $m^{-1}$), and reached minimum values during SSI (7 min, 3.4 s $m^{-1}$). These results indicated that SFI provided the strongest SRP retention potential in the storage zone. Notably, $q_s$ was highest during SSI (0.97 $m^2$ $s^{-1}$) and lower during ASI and SFI. Overall, SRP residence times in both the main channel and the storage zone were shortest during SSI, characterized by rapid transport and exchange, whereas SFI and ASI were more favorable for SRP retention.

### 3.3. SRP retention contribution in the main channel and the storage zone

Overall, SRP retention declined progressively from SFI to SSI (Fig. 5a). Retention was highest during SFI (8.3%–17.8%), decreased during ASI (4.6%–6.9%), and reached its lowest levels during SSI (1.3%–4.4%), consistent with the variation in SRP retention potential described in Section 3.2.

Across all periods, SRP retention in both the main channel and the storage zone closely followed the overall retention pattern. However, the contribution ratios of the two zones displayed contrasting trends (Fig. 5b). During SFI, the storage zone contributed nearly as much as the main channel, accounting for 35.9%–58.4% of total SRP retention. In ASI and SSI, dominance shifted toward the main channel, with its contribution increased to 53.5%–72.9% during ASI and exceeded 73% following dredging in SSI. Meanwhile, the storage zone's contribution declined to its annual minimum (19.9%–26.7%) (Fig. 5b), indicating that the main channel became the dominant contributor to SRP retention.

### 3.4. Contribution ratios of different mechanisms to SRP retention

Sampling site E was selected as a representative case to evaluate SRP responses to different retention scenarios in the main channel and the storage zone across the three study periods (Supplementary Fig. S2). Similar response patterns were observed in both hydraulic zones. Compared with Scenario 1, scenarios accounting for biological uptake and assimilation or adsorption produced lower peak SRP concentrations and more rapid attenuation, whereas scenarios excluding these processes resulted in higher concentrations and prolonged persistence. These results indicate that biological uptake and assimilation, together with adsorption, were important contributors to SRP retention in both the main channel and the storage zone.

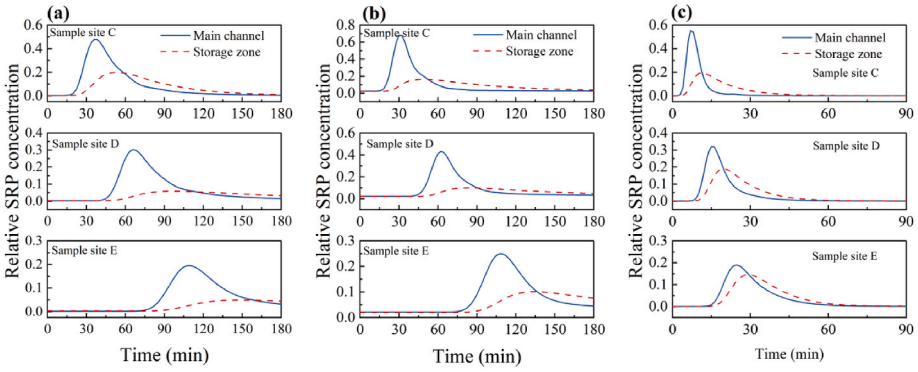


**Fig. 4.** Simulated breakthrough curves of relative SRP concentration in the main channel and storage zone at sampling sites C, D, and E. Values represent the ratio of concentration ($C$) at each sample site to the maximum concentration observed at the upstream boundary ($C_{B'max}$). Panels: (a) SFI (the fifth irrigation event, occurring in summer), (b) ASI (the sixth irrigation event, occurring in autumn), (c) SSI (the second irrigation event, occurring in spring).

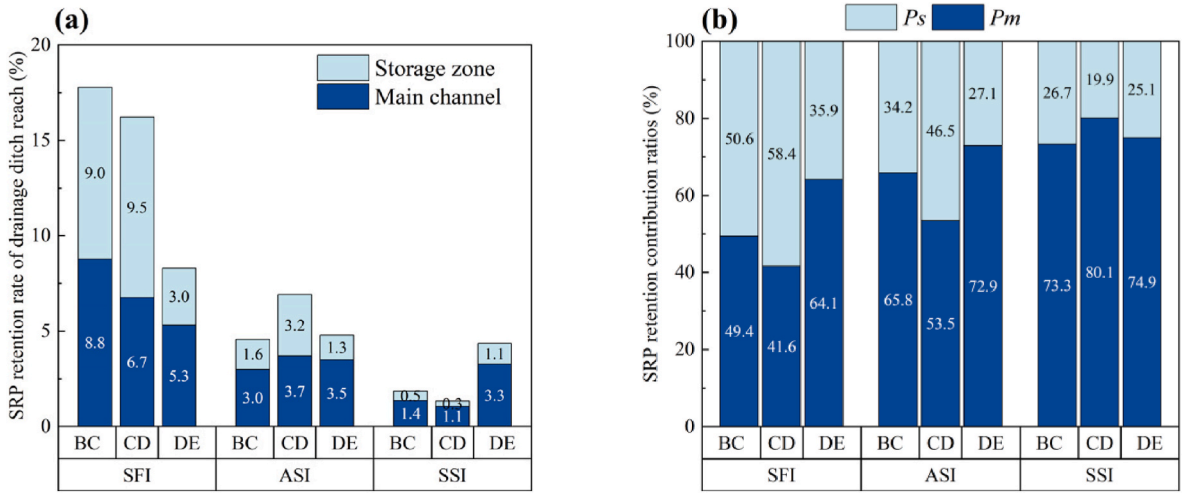


**Fig. 5.** SRP retention contributions in the main channel and the storage zone. (a) SRP retention rates of drainage ditch reaches, including contributions from both the main channel and the storage zone. (b) SRP retention contribution ratios of the main channel and storage zone for each ditch reach ($P_m$ and $P_s$, respectively).

During SFI and ASI, biological uptake and assimilation represented the dominant retention mechanism in both zones. In the main channel, its contribution $P_{m,biotic}$ remained consistently high across all periods (38–55%). In contrast, its contribution $P_{s,biotic}$ in the storage zone declined from 30% during SFI to 11% during SSI, coinciding with reductions in the storage zone area associated with vegetation senescence and dredging, as well as increased flow velocity. Notably, the importance of adsorption increased progressively from SFI to SSI. During SSI, adsorption accounted for 13% and 38% of SRP retention in the main channel and the storage zone, respectively, thereby becoming the dominant retention mechanism under post-dredging conditions. The contribution of hydrological processes was generally minor, reaching 16% only in the SFI storage zone and becoming nearly negligible under the high-flow conditions of SSI (Fig. 6).

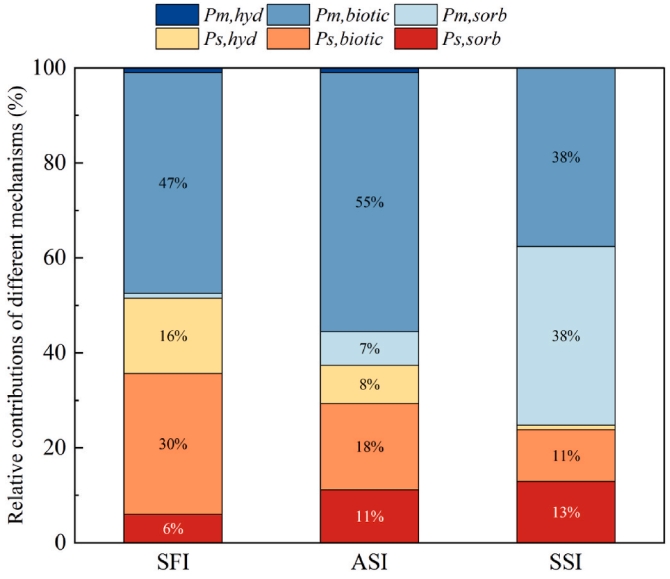


**Fig. 6.** Relative contributions of different mechanisms to SRP retention across different periods, including hydrological processes ($P_{m,hyd}$ and $P_{s,hyd}$, representing the main channel and storage zone, respectively), biological uptake and assimilation ($P_{m,biotic}$ and $P_{s,biotic}$), and adsorption ($P_{m,sorb}$ and $P_{s,sorb}$). SFI: the fifth irrigation event, occurring in summer; ASI: the sixth irrigation event, occurring in autumn; SSI: the second irrigation event, occurring in spring.

## 4. Discussion

### 4.1. Effects of channel condition changes on SRP retention

Hydrodynamics and nutrient cycling in small watercourses, such as drainage ditches, are highly sensitive to external factors, including runoff, seasonal fluctuations, and human-induced dredging (Gao et al., 2025). Our results indicate that seasonal variation and dredging alter channel morphology, vegetation cover, and hydrodynamic conditions (Table 1), thereby influencing phosphorus retention capacity.

Lower flow velocities generally favor phosphorus retention, as they prolong solute residence time and increase the likelihood of biological uptake, transformation, and physicochemical reactions (Liu et al., 2013; Schulz et al., 2003; Wan et al., 2024). During the SFI period, channel vegetation was well developed, and the storage zone accounted for a relatively large proportion of the total channel area. Under these conditions, flow velocity was low, while residence times in both the main channel ($T_c$) and storage zone ($T_s$) were the longest among the three study periods (Table 2). Vegetation can increase hydraulic roughness, while rooted macrophytes such as *Phragmites* may enhance rhizosphere activity and stimulate microbial processes involved in phosphorus retention (Cui et al., 2020; Lai et al., 2011; Vereecken et al., 2006). These conditions were associated with the highest SRP retention during SFI (Fig. 5a). However, phosphorus retention by vegetation is not simply proportional to vegetation cover but is also regulated by the overall metabolic state of the ecosystem (Feijoó et al., 2011).

In contrast, SRP retention was lowest during the post-dredging SSI period. Dredging reduced vegetation cover and storage-zone area while increasing flow velocity, which may have shortened phosphorus residence times and reduced retention efficiency. It may also disrupt biological habitats, biofilm development, and sediment physicochemical properties, weakening phosphorus retention and transformation processes (Licursi and Gómez, 2009; Moore et al., 2017). Furthermore, recovery of ecological functions following dredging may require considerable time (Guo et al., 2024).

Similar effects have been reported elsewhere. For example, dredging of the Imboassica River in Brazil reduced phosphorus retention capacity and increased downstream phosphorus transport, thereby elevating eutrophication risk (Marotta et al., 2009). However, in systems with heavily phosphorus-enriched sediments, dredging can temporarily improve water quality by removing phosphorus-rich deposits and reducing internal phosphorus release (Q. Zhang et al., 2025). Such benefits depend largely on effective control of external phosphorus inputs; otherwise, continued phosphorus loading may rapidly offset the

improvements achieved through dredging (Liu et al., 2016). These findings suggest that the influence of dredging on phosphorus cycling is highly context-dependent.

### 4.2. Contribution of SRP retention and shift in dominant mechanisms

Due to the heterogeneity of ditch hydrodynamics and channel conditions, both the relative contributions and dominant mechanisms of phosphorus retention differed between the main channel and the storage zone. The storage zone is generally regarded as a near-stationary hydraulic environment, where nutrients may be more readily retained through biological uptake and assimilation, as well as adsorption processes (DeAngelis et al., 1995). However, our results show that the main channel contributed more to SRP retention than the storage zone (Fig. 5b). This pattern may be related to differences in residence time, which is a key factor controlling nutrient retention (O'Connor et al., 2010; Zhao et al., 2024). In all three experiments, $T_c$ was consistently longer than $T_s$ (Table 2). In addition, the storage zone contribution increased with its proportion of total channel cross-sectional area, consistent with previous findings (Bohrman and Strauss, 2018).

The storage zone is also characterized by high biological activity. Vegetation rhizospheres, biofilms, and sediment pore communities provide favorable conditions for phosphorus uptake and transformation (Gooseff et al., 2007; Herzon and Helenius, 2008; Zhang et al., 2024). Consistent with these observations, biological uptake and assimilation were identified as the dominant SRP retention mechanism in the storage zone during SFI and ASI (Fig. 6). In the main channel, biological uptake also played a major role, likely facilitated by benthic algae and sediment-associated biofilms (McKnight et al., 2004; Runkel, 2007).

From SFI to SSI, fine sediment fractions increased from 65.9% to 81.0%, which may enhance phosphorus adsorption due to the associated increase in specific surface area and reactive binding sites (Meng et al., 2014; Wang et al., 2020; Yao et al., 2016). In addition, sediment total phosphorus (TP) concentrations decreased from 845.3 mg/kg during SFI and 871.1 mg/kg during ASI to 811.9 mg/kg during SSI, indicating reduced phosphorus saturation after dredging. Dredging likely exposed more reactive, low-P sediments and enhanced sediment–water exchange under higher flow velocity, thereby strengthening adsorption processes (D. R. Smith and C. Huang, 2010; Wan et al., 2024; Yu et al., 2017). It may also alter sediment–water interface conditions, oxygen availability, and phosphorus speciation, increasing the relative importance of adsorption in both channel zones during SSI (Wen et al., 2020).

### 4.3. Implications for drainage ditch management and ecological restoration

Optimized management of agricultural drainage ditches should shift from a sole focus on drainage efficiency to an integrated approach that balances drainage and ecological functions (Clifford et al., 2025). The results of this study indicate that seasonal variation and dredging affect phosphorus retention by altering channel structure and the relative roles of the main channel and storage zone, highlighting the importance of maintaining functional storage areas for sustaining phosphorus buffering capacity.

From a management perspective, excessive dredging should be avoided. Although dredging can restore hydraulic capacity, it may reduce storage-zone function and shorten residence time, thereby weakening phosphorus retention (Licursi and Gómez, 2009; Moore et al., 2017). Moderate interventions and ecological measures, such as riparian vegetation restoration and floating vegetation systems, are recommended to enhance nutrient retention at the landscape scale (Manolaki et al., 2020; Zhao et al., 2021).

At the policy level, drainage system management should incorporate indicators of nutrient retention and ecological function. Adaptive dredging strategies considering seasonal and channel conditions can help balance drainage efficiency and water-quality protection, supporting watershed-scale eutrophication control.

### 4.4. Limitations and future research

Although this study combined tracer experiments with the OTIS model to investigate phosphorus retention characteristics and mechanisms under different channel conditions, several limitations should be acknowledged. The OTIS model uses a simplified two-compartment framework, and biological uptake and assimilation are represented by first-order reaction coefficients. In addition, lateral inflow was assumed to be negligible. While these assumptions help identify dominant retention mechanisms, they may not fully capture the complex hydrodynamic and biogeochemical processes in natural drainage ditches. Some uncertainty also remains due to parameter estimation through inverse modeling.

Only three tracer experiments were conducted in a representative drainage ditch in the Hetao Irrigation District. Given the spatial variability in hydrology, vegetation, sediment properties, and phosphorus loading among ditches, the broader applicability of the results requires further validation. Moreover, the identification of dominant mechanisms was mainly based on model scenario analysis and lacks direct evidence from microbial, biofilm, and adsorption measurements. Future work should include targeted experiments to further validate these mechanisms.

Finally, this study focused on short-term effects of dredging, and its long-term impacts on channel ecological structure and phosphorus retention require further investigation.

## 5. Conclusions

This study combined tracer experiments with numerical simulations to reveal the effects of seasonal variations and dredging on phosphorus retention processes in agricultural drainage ditches. The results indicate that the relative contributions of the main channel and storage zone, as well as the dominant retention mechanisms, undergo marked shifts as channel conditions change. During summer and autumn, when vegetation cover is high and biological activity is strong, phosphorus retention is likely governed primarily by biological uptake and assimilation. In contrast, after dredging, overall phosphorus retention capacity decreases, the contribution of the main channel increases, and retention processes tend to shift toward adsorption-dominated mechanisms. These findings highlight the importance of maintaining functional storage zones and their ecological structure for enhancing phosphorus retention in agricultural drainage ditches. Therefore, ditch management should ensure adequate drainage capacity while avoiding frequent or excessive dredging, and ecological functions should be preserved by maintaining flow-slowing and temporary storage areas and restoring vegetation. This study provides a scientific basis for ecological management of agricultural drainage systems, control of agricultural nonpoint source pollution, and mitigation of watershed eutrophication.

## CRediT authorship contribution statement

**Jiahui Wang:** Data curation, Formal analysis, Investigation, Software, Visualization, Writing – original draft. **Minghong Chen:** Conceptualization, Funding acquisition, Methodology, Project administration, Resources, Supervision, Writing – review & editing. **Minghui Qiu:** Data curation. **Fengchu Wang:** Investigation. **Xuanye Liu:** Investigation. **Chaozi Wang:** Methodology, Writing – review & editing. **Zailin Huo:** Funding acquisition.

## Declaration of competing interests

The authors declare that they have no known competing financial interests or personal relationships that could have appeared to influence the work reported in this paper.

## Acknowledgements

This work was supported by the National Natural Science Foundation of China [Grant No. 52130902, 52479053].

## Appendix A. Supplementary data

Supplementary data to this article can be found online at https://doi.org/10.1016/j.jenvman.2026.130715.

## Data availability

Data will be made available on request.

## References

Bencala, K.E., Walters, R.A., 1983. Simulation of solute transport in a Mountain pool-and-riffle stream: a transient storage model. Water Resour. Res. 19, 718–724. https://doi.org/10.1029/WR019i003p00718.

Bieroza, M., Hallberg, L., Livsey, J., Prischl, L.-A., Wynants, M., 2024. Recognizing agricultural headwaters as critical ecosystems. Environ. Sci. Technol. 58, 4852–4858. https://doi.org/10.1021/acs.est.3c10165.

Bohrman, K.J., Strauss, E.A., 2018. Macrophyte-driven transient storage and phosphorus uptake in a Western Wisconsin stream. Hydrol. Process. 32, 253–263. https://doi.org/10.1002/hyp.11411.

Bukaveckas, P.A., 2007. Effects of channel restoration on water velocity, transient storage, and nutrient uptake in a channelized stream. Environ. Sci. Technol. 41, 1570–1576. https://doi.org/10.1021/es061618x.

Chen, M., Li, Y., Wang, C., Walter, M.T., 2022. An investigation of the effects of humic acid on soil erosion and loss of phosphorus from soil to runoff: experiment and modeling. Geoderma 427, 116121. https://doi.org/10.1016/j.geoderma.2022.116121.

Clifford, C., Bieroza, M., Clarke, S.J., Pickard, A., Stratigos, M.J., Hill, M.J., Raheem, N., Tatariw, C., Wood, P.J., Arismendi, I., Audet, J., Aviles, D., Bergman, J.N., Brown, A. G., Burns, R.E., Connolly, J., Cook, S., Crabot, J., Cross, W.F., Dean, J.F., Evans, C.D., Fenton, O., Friday, L., Gething, K.J., Giannico, G., Habib, W., Hasselquist, E.M., Heili, N.M., Van Der Knaap, J., Kosten, S., Law, A., Van Der Lee, G.H., Mathers, K.L., Morgan, J.E., Rahimi, H., Sayer, C.D., Schepers, M., Shaw, R.F., Smiley, P.C., Speir, S.L., Strock, J.S., Struik, Q., Tank, J.L., Wang, H., Webb, J.R., Webster, A.J., Yan, Z., Zivec, P., Peacock, M., 2025. Lines in the landscape. Commun. Earth Environ. 6, 693. https://doi.org/10.1038/s43247-025-02699-y.

Conley, D.J., Paerl, H.W., Howarth, R.W., Boesch, D.F., Seitzinger, S.P., Havens, K.E., Lancelot, C., Likens, G.E., 2009. Controlling eutrophication: Nitrogen and phosphorus. Science 323, 1014–1015. https://doi.org/10.1126/science.1167755.

Cui, N., Zhang, X., Cai, M., Zhou, L., Chen, G., Zou, G., 2020. Roles of vegetation in nutrient removal and structuring microbial communities in different types of agricultural drainage ditches for treating farmland runoff. Ecol. Eng. 155, 105941. https://doi.org/10.1016/j.ecoleng.2020.105941.

De Oliveira, L.E.D., Yamasaki, T.N., Janzen, J.G., Gualtieri, C., 2024. Effects of vegetation density on flow, mass exchange and sediment transport in lateral cavities. J. Hydrol. 632, 130910. https://doi.org/10.1016/j.jhydrol.2024.130910.

DeAngelis, D.L., Loreau, M., Neergaard, D., Mulholland, P.J., Marzolf, E.R., 1995. Modelling nutrient-periphyton dynamics in streams: the importance of transient storage zones. Ecol. Model. 80, 149–160. https://doi.org/10.1016/0304-3800(94)00066-Q.

Feijoó, C., Giorgi, A., Ferreiro, N., 2011. Phosphate uptake in a macrophyte-rich pampean stream. Limnologica 41, 285–289. https://doi.org/10.1016/j.limno.2010.11.002.

Field, H.R., Sawyer, A.H., Welch, S.A., Benefiel, R.K., Mathie, D.M., Hood, J.M., Pawlowski, E.D., Karwan, D.L., Kreiling, R.M., Johnson, Z.I., Hanrahan, B.R., King, K.W., 2023. Importance of dense aquatic vegetation in seasonal phosphate and particle transport in an agricultural headwater stream. Water Resour. Res. 59, e2022WR033782. https://doi.org/10.1029/2022WR033782.

Gao, X., Bi, Y., Su, L., Lei, Y., Gong, L., Dong, X., Li, X., Yan, Z., 2024. Unveiling the nitrogen and phosphorus removal potential: comparative analysis of three coastal wetland plant species in lab-scale constructed wetlands. J. Environ. Manag. 351, 119864. https://doi.org/10.1016/j.jenvman.2023.119864.

Gao, Y., Wang, P., Hu, B., Qian, J., Jin, Q., Li, Q., 2025. Unraveling multiple effects of environmental factors on nutrient release: towards optimal conditions in agricultural drainage ditches. J. Environ. Sci. 158, 542–554. https://doi.org/10.1016/j.jes.2025.03.017.

Giri, S., 2021. Water quality prospective in twenty first century: status of water quality in major river basins, contemporary strategies and impediments: a review. Environ. Pollut. 271, 116332. https://doi.org/10.1016/j.envpol.2020.116332.

Gooseff, M.N., Hall, R.O., Tank, J.L., 2007. Relating transient storage to channel complexity in streams of varying land use in jackson hole, wyoming. Water Resour. Res. 43, 2005WR004626. https://doi.org/10.1029/2005WR004626.

Guo, G., Lapen, D.R., Khan, I.U.H., Sunohara, M., Craiovan, E., Chen, W., 2024. Examining the impact of agricultural drainage ditch management on in-stream bacterial communities involved in nitrogen cycling: insights from the environmental change one health observatory (ECO2). Front. Sustain. Food Syst. 8, 1329422. https://doi.org/10.3389/fsufs.2024.1329422.

Harvey, J., Gooseff, M., 2015. River corridor science: hydrologic exchange and ecological consequences from bedforms to basins: river corridors from bedforms to basins. Water Resour. Res. 51, 6893–6922. https://doi.org/10.1002/2015WR017617.

Harvey, J.W., Wagner, B.J., 2000. Quantifying hydrologic interactions between streams and their subsurface hyporheic zones. In: Streams and Ground Waters. Elsevier, pp. 3–44. https://doi.org/10.1016/B978-012389845-6/50002-8.

Harvey, J.W., Wagner, B.J., Bencala, K.E., 1996. Evaluating the reliability of the stream tracer approach to characterize stream-subsurface water exchange. Water Resour. Res. 32, 2441–2451. https://doi.org/10.1029/96WR01268.

Herzon, I., Helenius, J., 2008. Agricultural drainage ditches, their biological importance and functioning. Biol. Conserv. 141, 1171–1183. https://doi.org/10.1016/j.biocon.2008.03.005.

Ho, J.C., Michalak, A.M., Pahlevan, N., 2019. Widespread global increase in intense lake phytoplankton blooms since the 1980s. Nature 574, 667–670. https://doi.org/10.1038/s41586-019-1648-7.

Hu, F., Yang, H., Zhou, X., Zhao, S., Qiu, L., Wei, S., Wang, X., Hu, J., Chen, Y., Hu, H., Zhou, H., 2026. Pollution transfer and environmental health implications: network evolution and proximity mechanisms in the yangtze river delta, China. Front. Public Health 14, 1770901. https://doi.org/10.3389/fpubh.2026.1770901.

Ji, K., Li, W., Hao, X., Ouyang, W., Zhang, Y., 2024. Transport dynamics of watershed discharged diffuse phosphorus pollution load to the lake in middle of yangtze river basin. Environ. Pollut. 344, 123221. https://doi.org/10.1016/j.envpol.2023.123221.

Karl, D.M., 2014. Microbially mediated transformations of phosphorus in the sea: new views of an old cycle. Ann. Rev. Mar. Sci 6, 279–337. https://doi.org/10.1146/annurev-marine-010213-135046.

Lai, W., Wang, S., Peng, C., Chen, Z., 2011. Root features related to plant growth and nutrient removal of 35 wetland plants. Water Res. 45, 3941–3950. https://doi.org/10.1016/j.watres.2011.05.002.

Li, C., Lu, X., Chen, J., Tan, Q., Luo, G., Wu, L., Chen, F., Ran, C., Zhang, S., Xiong, L., Du, C., Song, F., Xiao, B., Li, Z., Xue, Y., Long, M., Bai, X., 2025. Silicate chemical weathering disrupts the global patterns of phosphorus limitation. Nat. Commun. 16, 10742. https://doi.org/10.1038/s41467-025-65773-1.

Li, H., Xu, Y., Wei, Y., Zhang, M., Zhou, J., 2025. Effect of sediment on fluvial phosphorus and aquatic water quality. J. Environ. Manag. 379, 124722. https://doi.org/10.1016/j.jenvman.2025.124722.

Li, X., Zhang, W., Wu, J., Li, H., Zhao, T., Zhao, C., Shi, R., Li, Z., Wang, C., Li, C., 2021. Loss of nitrogen and phosphorus from farmland runoff and the interception effect of an ecological drainage ditch in the north China plain—a field study in a modern agricultural park. Ecol. Eng. 169, 106310. https://doi.org/10.1016/j.ecoleng.2021.106310.

Licursi, M., Gómez, N., 2009. Effects of dredging on benthic diatom assemblages in a lowland stream. J. Environ. Manag. 90, 973–982. https://doi.org/10.1016/j.jenvman.2008.03.004.

Liu, C., Li, R., Fu, Y., 2022. Nutrient retention in agricultural headwater stream: artificial manipulation of main-channel morphology and hydrologic condition. Environ. Sci. Pollut. Res. 29, 83004–83019. https://doi.org/10.1007/s11356-022-21660-6.

Liu, C., Zhong, J., Wang, J., Zhang, L., Fan, C., 2016. Fifteen-year study of environmental dredging effect on variation of nitrogen and phosphorus exchange across the sediment-water interface of an urban lake. Environ. Pollut. 219, 639–648. https://doi.org/10.1016/j.envpol.2016.06.040.

Liu, F., Xiao, R., Wang, Y., Li, Y., Zhang, S., Luo, Q., Wu, J., 2013. Effect of a novel constructed drainage ditch on the phosphorus sorption capacity of ditch soils in an agricultural headwater catchment in subtropical central China. Ecol. Eng. 58, 69–76. https://doi.org/10.1016/j.ecoleng.2013.06.008.

Liu, Ji, Wang, Y., Li, Yong, Peñuelas, J., Zhao, Y., Sardans, J., Tetzlaff, D., Liu, Jian, Liu, X., Yuan, H., Li, Yanyan, Chen, J., Wu, J., 2023. Soil ecological stoichiometry synchronously regulates stream nitrogen and phosphorus concentrations and ratios. Catena 231, 107357. https://doi.org/10.1016/j.catena.2023.107357.

Manolaki, P., Mouridsen, M.B., Nielsen, E., Olesen, A., Jensen, S.M., Lauridsen, T.L., Baattrup-Pedersen, A., Sorrell, B.K., Riis, T., 2020. A comparison of nutrient uptake efficiency and growth rate between different macrophyte growth forms. J. Environ. Manag. 274, 111181. https://doi.org/10.1016/j.jenvman.2020.111181.

Marotta, H., Bento, L., Esteves, F.D.A., Enrich-Prast, A., 2009. Whole ecosystem evidence of eutrophication enhancement by wetland dredging in a shallow tropical Lake. Estuaries Coasts 32, 654–660. https://doi.org/10.1007/s12237-009-9152-1.

McKnight, D.M., Runkel, R.L., Tate, C.M., Duff, J.H., Moorhead, D.L., 2004. Inorganic N and P dynamics of antarctic glacial meltwater streams as controlled by hyporheic exchange and benthic autotrophic communities. J. North Am. Benthol. Soc. 23, 171–188. https://doi.org/10.1899/0887-3593(2004)023%3C0171:INAPDO%3E2.0.CO;2.

Meng, J., Yao, Q., Yu, Z., 2014. Particulate phosphorus speciation and phosphate adsorption characteristics associated with sediment grain size. Ecol. Eng. 70, 140–145. https://doi.org/10.1016/j.ecoleng.2014.05.007.

Moore, M., Locke, M.A., Jenkins, M., Steinriede, R.W., McChesney, D.S., 2017. Dredging effects on selected nutrient concentrations and ecoenzymatic activity in two drainage ditch sediments in the lower mississippi river valley. Int. Soil Water Conserv. Res. 5, 190–195. https://doi.org/10.1016/j.iswcr.2017.06.004.

Nsenga Kumwimba, M., Meng, F., Iseyemi, O., Moore, M.T., Zhu, B., Tao, W., Liang, T.J., Ilunga, L., 2018. Removal of non-point source pollutants from domestic sewage and agricultural runoff by vegetated drainage ditches (VDDs): design, mechanism, management strategies, and future directions. Sci. Total Environ. 639, 742–759. https://doi.org/10.1016/j.scitotenv.2018.05.184.

O'Connor, B.L., Hondzo, M., Harvey, J.W., 2010. Predictive modeling of transient storage and nutrient uptake: implications for stream restoration. J. Hydraul. Eng. 136, 1018–1032. https://doi.org/10.1061/(ASCE)HY.1943-7900.0000180.

Reid, A.J., Carlson, A.K., Creed, I.F., Eliason, E.J., Gell, P.A., Johnson, P.T.J., Kidd, K.A., MacCormack, T.J., Olden, J.D., Ormerod, S.J., Smol, J.P., Taylor, W.W., Tockner, K., Vermaire, J.C., Dudgeon, D., Cooke, S.J., 2019. Emerging threats and persistent conservation challenges for freshwater biodiversity. Biol. Rev. 94, 849–873. https://doi.org/10.1111/brv.12480.

Riza, M., Ehsan, M.N., Pervez, M.N., Khyum, M.M.O., Cai, Y., Naddeo, V., 2023. Control of eutrophication in aquatic ecosystems by sustainable dredging: effectiveness, environmental impacts, and implications. Case Stud. Chem. Environ. Eng. 7, 100297. https://doi.org/10.1016/j.cscee.2023.100297.

Runkel, R.L., 1998. One-dimensional transport with inflow and storage (OTIS): a solute transport model for streams and rivers. U.S. Geological Survey Water-Resources Investigations Report 98–4018. https://doi.org/10.3133/wri984018.

Runkel, R.L., 2002. A new metric for determining the importance of transient storage. J. North Am. Benthol. Soc. 21, 529–543. https://doi.org/10.2307/1468428.

Runkel, R.L., 2007. Toward a transport-based analysis of nutrient spiraling and uptake in streams. Limnol Oceanogr. Methods 5, 50–62. https://doi.org/10.4319/lom.2007.5.50.

Runkel, R.L., McKnight, D.M., Bencala, K.E., Chapra, S.C., 1996. Reactive solute transport in streams: 2. Simulation of a pH modification experiment. Water Resour. Res. 32, 419–430. https://doi.org/10.1029/95WR03107.

Schulz, M., Kozerski, H.-P., Pluntke, T., Rinke, K., 2003. The influence of macrophytes on sedimentation and nutrient retention in the lower river spree (Germany). Water Res. 37, 569–578. https://doi.org/10.1016/S0043-1354(02)00276-2.

Shigaki, F., Kleinman, P.J.A., Schmidt, J.P., Sharpley, A.N., Allen, A.L., 2008. Impact of dredging on phosphorus transport in agricultural drainage ditches of the Atlantic coastal Plain[1]. JAWRA J. Am. Water Resour. Assoc. 44, 1500–1511. https://doi.org/10.1111/j.1752-1688.2008.00254.x.

Smith, D.R., Huang, C., 2010. Assessing nutrient transport following dredging of agricultural drainage ditches. Trans. ASABE 53, 429–436. https://doi.org/10.13031/2013.29583.

Vereecken, H., Baetens, J., Viaene, P., Mostaert, F., Meire, P., 2006. Ecological management of aquatic plants: effects in lowland streams. Hydrobiologia 570, 205–210. https://doi.org/10.1007/s10750-006-0181-5.

Vymazal, J., Březinová, T.D., 2018. Removal of nutrients, organics and suspended solids in vegetated agricultural drainage ditch. Ecol. Eng. 118, 97–103. https://doi.org/10.1016/j.ecoleng.2018.04.013.

Wan, H., Huang, Y., Cheng, X., Feng, J., Li, R., 2024. Experimental research on the effect of water velocity on phosphorus release from sediments of a Plateau cold water type river. J. Contam. Hydrol. 261, 104285. https://doi.org/10.1016/j.jconhyd.2023.104285.

Wang, X., Zhou, J., Wu, Yanhong, Bol, R., Wu, Yong, Sun, H., Bing, H., 2020. Fine sediment particle microscopic characteristics, bioavailable phosphorus and environmental effects in the world largest reservoir. Environ. Pollut. 265, 114917. https://doi.org/10.1016/j.envpol.2020.114917.

Wen, S., Zhong, J., Li, X., Liu, C., Yin, H., Li, D., Ding, S., Fan, C., 2020. Does external phosphorus loading diminish the effect of sediment dredging on internal phosphorus loading? An in-situ simulation study. J. Hazard Mater. 394, 122548. https://doi.org/10.1016/j.jhazmat.2020.122548.

Xiang, H., Li, X., Xiao, R., Chen, J., Dai, W., 2024. Is dredging an effective ecological restoration method to improve water quality in freshwater ecosystems? Ecol. Eng. 209, 107425. https://doi.org/10.1016/j.ecoleng.2024.107425.

Yao, Q.-Z., Du, J.-T., Chen, H.-T., Yu, Z.-G., 2016. Particle-size distribution and phosphorus forms as a function of hydrological forcing in the yellow river. Environ. Sci. Pollut. Res. 23, 3385–3398. https://doi.org/10.1007/s11356-015-5567-3.

Yu, J., Ding, S., Zhong, J., Fan, C., Chen, Q., Yin, H., Zhang, L., Zhang, Y., 2017. Evaluation of simulated dredging to control internal phosphorus release from sediments: focused on phosphorus transfer and resupply across the sediment-water interface. Sci. Total Environ. 592, 662–673. https://doi.org/10.1016/j.scitotenv.2017.02.219.

Zarnetske, J.P., Gooseff, M.N., Brosten, T.R., Bradford, J.H., McNamara, J.P., Bowden, W.B., 2007. Transient storage as a function of geomorphology, discharge, and permafrost active layer conditions in arctic tundra streams. Water Resour. Res. 43, 2005WR004816. https://doi.org/10.1029/2005WR004816.

Zhang, J., Geng, Y., Li, Z., Li, P., Wang, T., Xu, G., Yu, K., Wang, W., Wang, P., Guo, M., 2025. Modeling sediment flux in river confluences: a comprehensive momentum-based study. Water Resour. Res. 61, e2024WR039154. https://doi.org/10.1029/2024WR039154.

Zhang, J., Yan, M., Lu, X., Wang, T., 2024. Nutrient removal performance from agricultural drainage by strengthening ecological ditches in hilly areas. Agric. Water Manag. 291, 108623. https://doi.org/10.1016/j.agwat.2023.108623.

Zhang, K., Li, M., Qu, S., Zhao, Y., Duan, L., Yang, X., Li, D., Liao, Z., Yu, R., 2025. Spatio-seasonal variability of source contributions to water quality in a large irrigation drainage lake basin based on the entropy weighted quality index, positive matrix factorization, and isotopic tracers. Environ. Pollut. 382, 126670. https://doi.org/10.1016/j.envpol.2025.126670.

Zhang, Q., Huang, J., Ji, Y., Zhang, J., Zhang, S., Gao, J., 2025. How sediment dredging alters phosphorus dynamics in a lowland rural river? J. Environ. Sci. 147, 189–199. https://doi.org/10.1016/j.jes.2023.09.030.

Zhao, B., Zeng, Q., Wang, J., Jiang, Y., Liu, H., Yan, L., Yang, Z., Yang, Q., Zhang, F., Tang, J., Hu, P., 2024. Impact of cascade reservoirs on nutrients transported downstream and regulation method based on hydraulic retention time. Water Res. 252, 121187. https://doi.org/10.1016/j.watres.2024.121187.

Zhao, D., Chen, C., Yang, J., Zhou, S., Du, J., Zhang, M., An, S., 2021. Mutual promotion of submerged macrophytes and biofilms on artificial macrophytes for nitrogen and COD removal improvement in eutrophic water. Environ. Pollut. 277, 116718. https://doi.org/10.1016/j.envpol.2021.116718.